Mechanical Properties of Thermoplastic Polymers in Fused Filament Fabrication (FFF)

Nancy Bhardwaj[1], Hani Henein [1], Tonya Wolfe [2]

[1]Advanced Materials and Processing Laboratory (AMPL), Department of Chemical and Materials Engineering, University of Alberta, Canada
[2]Red Deer Polytechnic, Red Deer, Canada

Abstract

Fused filament fabrication (FFF) is a method used to fabricate initial prototypes out of polymeric materials with printed parts often being used as load carrying elements. The mechanical properties of various polymer materials produced under certain printing conditions exhibit superior strength and ductility and may serve as an inexpensive replacement for metal or wooden parts. To gain knowledge of 3-D printed part strength and compare the quality of filament material from several manufacturers, this study characterizes the mechanical properties of parts printed from various commercial FFF feedstocks. Uniaxial tensile testing is performed to determine the ultimate tensile strength, Youngs modulus and fracture strain, of polymer and composite materials.

Keywords: additive manufacturing, thermoplastic polymer, fused deposition modeling, material characterization, 3D printing, extrusion, composites

1. Introduction

Fused filament fabrication (FFF) is an additive manufacturing (AM) technology that allows for the creation of complex three-dimensional (3D) functional prototypes. 3D parts of complex geometries are fabricated using a layer-by-layer material extrusion process, based solely on a 3D computer-aided design (CAD) model (Górski et al., 2013). The FFF process, commonly referred to as 3D printing, consists of feeding a feedstock filament material into a heated extruder, heating the material to create a flowable feedstock which is uniformly deposited onto the surface of a printing platform. FFF can produce finished parts with good surface quality, dimensional stability, and mechanical properties for a wide range of materials (Bellini & Güçeri, 2003). It has gained popularity in recent years as a reliable and economical method for manufacturing, allowing for the adoption of this technology for depositing a wide range of materials including polymers, metals, and even composites. As a result, this method has expanded into use in biomedical technology, aerospace, automotive and surface engineering applications.

The properties of the most commonly used polymeric materials used in 3D printing using FFF are summarized in Table 1. Polylactic Acid (PLA) and Acrylonitrile Butadiene Styrene (ABS) are the two most widely investigated filament materials, referred to as standard plastics

used in non-critical engineering applications. Thermoplastic polymers for structural engineering applications include Polyethylene terephthalate (PET), Polyamide (PA) or Nylon, and Acrylonitrile styrene acrylate (ASA). Advanced polymers such as Polyetherimides (PEI) are specific to critical engineering applications where a combination of high mechanical, thermal, and chemical performance is required. Table 1 lists the key attributes of these polymer materials.

Table 1. Physical properties and key attributes of common FFF polymers

Material	Produced from	Structure	T_g (°C)	T_m (°C)	Pros	Cons
ABS	Petroleum	amorphous	105	150-323	tough, flexible, heat-resistant, low cost	toxic fumes & low UV resistance
ASA	Synthetic	amorphous	100	170-280	strong, tough, heat, water & UV-resistant	toxic fumes, expensive, high temperatures
PA (Nylon)	Synthetic	semi-crystalline	60-80	255	strong, tough, flexible, biocompatible, high thermal stability, impact & wear-resistant	hygroscopic
PET	Petroleum	amorphous	73	180-293	strong, chemical-resistant, high optical clarity, food safe, recyclable	hygroscopic
PEI	Synthetic	semi-crystalline	143	343	high weight-to-strength ratio, dielectric, chemical, heat, wear & flame-resistant	expensive & high temperatures
PLA	Plant starch	semi-crystalline	55	155	strong, biodegradable, low cost	brittle, hygroscopic, low UV resistance

The characteristics of FFF printed parts such as tensile strength, compressive strength, flexural strength, hardness, yield strength and ductility are of primary importance and will be described in the following sections.

3. Experimental

3.1 Materials

To investigate the tensile properties and failure mechanisms of FFF printed parts, a total of 28 different commercial filaments were printed and tested. The materials include various types of PLA, ABS, Polyolefin, PETG, Nylon, ASA, and PEI-based polymers. In addition to polymeric materials, several polymer-matrix composites (PMC) are tested. The composite filaments are reinforced with wood, glass, copper, and carbon fiber. Table 2 lists the characteristics of each filament, including: material type, supplier, color, and printing temperatures used.

Table 2. Important filament characteristics and processing temperatures

Name	Material Type	Supplier	Color	T_g (°C)	Nozzle (°C)	Bed (°C)
PLA1	PLA	A	Natural	60	220	60
PLA2		A	Gold	60		
PLA3		A	White	60		
PLA4		A	Orange	60		
PLA5		B	Black	55		
PLA6		C	White	55		
PLA/PHA1	PLA/PHA Blend	B	White	55		
PLA/PHA2		B	Green	55		
SilkPLA	Modified PLA	A	Blue			
ToughPLA		D	Blue	60		
AdvPLA		E	Natural	55		
ABS1	ABS	A	Natural	105	230	100
ABS2		F	Black	105	250	
PETG1	PETG	C	Natural	81	240	85
PETG2		C	Blue	81		
PETG3		G	Red	70	220	80
Copolyester	Modified PET	B	Black	85	240	85
Nylon1	Nylon	A	Natural	-	250	80
Nylon2	Nylon 6/6,6	H	Black	67		
Polyolefin	Polyolefin	I	Black		190	25
ASA	Modified ASA	F	Silver		250	90
PEI	PEI	J	Natural	217	375	113
WoodPLA	PMC	A	Brown	55	225	90
GlassPLA		F	Clear		215	60
CuPLA1		B	Copper		195	60
CuPLA2		K	Copper		195	60
CFPLA		A	Black		220	60
CFABS		C	Black		250	100

3.2 Sample Preparation

Tensile test bars of each material were printed according to dimensions stated in American Standard Test Method (ASTM) D638, the standard method for testing tensile properties of plastic materials. Figure 1 illustrates the profile of each tensile bar, with labelled dimensions (ASTM, 2014). The profile was drafted using Autodesk TinkerCAD, a three-dimensional computer aided design (CAD) platform and exported in STL format. Ultimaker Cura 3.4 3D slicing software was used to process the CAD model into horizontal layers and generate toolpaths to efficiently print each layer, in the form of a GCODE. Samples were printed using the Machina Mk2 FFF 3D printer, using processing parameters listed in Table 3. All tensile bars were printed using a nozzle 0.4mm

in diameter, except for the five PMC filaments which required a 0.8mm nozzle to print successfully. After printing, samples are stored at 23°C and 50% relative humidity for a minimum of 24 hours to homogenize before tensile testing. Six samples per material were printed for testing, apart from PLA/wood for which only three samples were printed due to filament shortage.

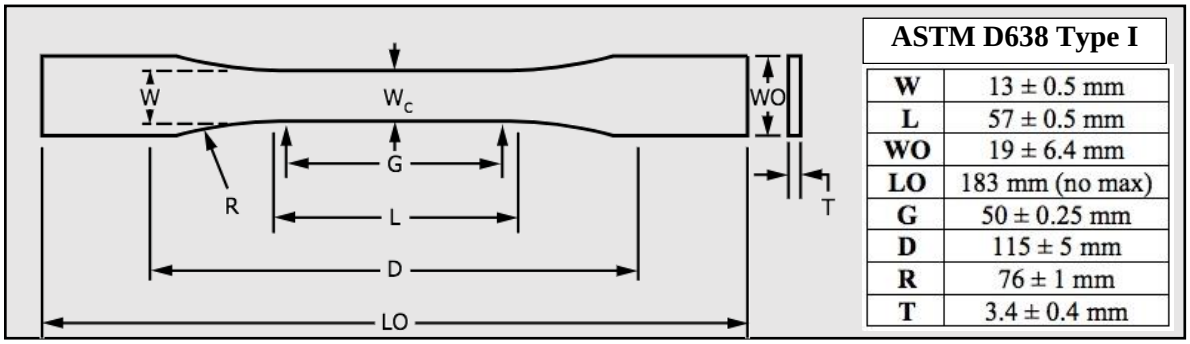

ASTM D638 Type I	
W	13 ± 0.5 mm
L	57 ± 0.5 mm
WO	19 ± 6.4 mm
LO	183 mm (no max)
G	50 ± 0.25 mm
D	115 ± 5 mm
R	76 ± 1 mm
T	3.4 ± 0.4 mm

Figure 1. ASTM D638 Type 1 Tensile Testing Specimen Adapted from (ASTM, 2014)

Table 3. Toolpath and process parameters for FDM

Toolpath Parameters				Process Parameters	
Initial layer height (mm)	0.18	Extrusion width (mm)	0.4-0.8	Filament diameter (mm)	1.75 ±0.05
Layer height (mm)	0.2	Infill overlap (%)	15	Nozzle diameter (mm)	0.4-0.8
Infill density (%)	100	Print Speed(mm)	60	Extrusion Multiplier	1
Infill pattern	Grid	Support type	brim	Cooling Fan	Off
Infill angle (°)	-45/45	Brim width (mm)	8	Build platform heating	On

3.3 Tensile Testing

The mechanical tensile properties of the printed polymeric samples were measured using the Instron 3366 Dual Column testing system. Each tensile specimen was tested using 114.3 mm grip separation with a crosshead speed of 5mm/min, a 50.8 mm extensometer, and a load cell of 10 kN All samples were pulled uniaxially until fracture. Mechanical properties including, ultimate tensile strength (UTS), Young's modulus (*E*) and fracture strain (**ε**l) were recorded.

4. Results and Discussion

Table 4-6 summarizes the tensile testing results, including the ultimate tensile strength (UTS), modulus (E), and fracture strain (el) of each tested material. The numerical values in Table 4-6 are representative of an average value with standard deviations included.

Table 4. Tensile results for PLA 3D-printed materials

Name	UTS (MPa)	Strain at Max load (%)	Elastic Modulus (GPa)	Fracture Stress (MPa)	Fracture Strain (%)
PLA1	51.7 ± 0.6	2.18	3.38 ± 0.15	50.21	2.77 ± 0.40
PLA2	45.8 ± 0.8	2.21	3.01 ± 0.06	39.80	4.15 ± 0.72
PLA3	43.5 ± 6.9	1.81	2.93 ± 0.23	32.76	1.45 ± 0.32
PLA4	47.8 ± 0.4	2.23	2.94 ± 0.03	36.76	5.76 ± 2.0
PLA5	51.8 ± 0.5	2.21	3.13 ± 0.03	37.00	6.58 ± 1.0
PLA6	47.3 ± 1.3	2.23	2.99 ± 0.06	43.14	3.63 ± 1.3
PLA/PHA1	32.8 ± 0.9	2.54	2.42 ± 0.05	29.45	5.64 ± 1.4
PLA/PHA2	48.6 ± 0.9	2.23	2.93 ± 0.05	41.23	5.46 ± 0.97
SilkPLA	30.7 ± 0.4	3.62	2.02 ± 0.04	4.65	46.5 ± 13.3
ToughPLA	53.3 ± 2.7	2.24	3.29 ± 0.09	51.48	3.58 ± 0.25
AdvPLA	42.7 ± 2.5	1.96	2.81 ± 0.07	21.98	4.31 ± 2.7

Table 5. Tensile results for ABS, PETG, and Copolyester 3D-printed materials

Name	UTS (MPa)	Strain at Max load (%)	Elastic Modulus (GPa)	Fracture Stress (MPa)	Fracture Strain (%)
ABS1	35.8 ± 0.8	2.76	2.06 ± 0.06	33.65	3.67 ± 0.59
ABS2	33.6 ± 0.9	2.51	1.96 ± 0.03	28.79	12.7 ± 6.8
PETG1	38.5 ± 3.0	3.56	1.76 ± 0.09	31.46	4.52 ± 0.81
PETG2	40.4 ± 1.7	3.66	1.79 ± 0.03	31.07	6.73 ± 2.6
PETG3	35.9 ± 4.1	3.45	1.67 ± 0.15	32.39	3.83 ± 0.50
Copolyester	43.6 ± 0.8	4.10	1.71 ± 0.05	25.82	10.6 ± 0.85

Table 6. Tensile results for ABS, PETG, and Copolyester 3D-printed materials

Name	UTS (MPa)	Strain at Max load (%)	Elastic Modulus (GPa)	Fracture Stress (MPa)	Fracture Strain (%)
Nylon1	52.8 ± 0.8	3.95	2.17 ± 0.02	7.18 ± 3.8	28.4 ± 15.1
Nylon2	63.0 ± 3.2	3.45	2.58 ± 0.05	55.1 ± 8.4	4.56 ± 1.7
ASA	37.1 ± 2.0	0.03	1.88 ± 0.05	32.25	0.04 ± 0.01
PEI	58.7 ± 2.0	0.06	1.53 ± 0.08	58.23	0.07 ± 0.01
Polyolefin	14.4 ± 0.1	0.20	0.47 ± 0.01	12.59	2.06 ± 1.1

4.1 Tensile Properties of Polymers

The tensile behavior of the PLA polymeric materials is shown in Figure 2. It is important to note that each stress-strain curve seen in Figure 2 represents the tensile data obtained from a single test sample, compared to the values in Table 4 which are an average of multiple tests.

Samples printed from PLA1-PLA6 had average tensile strengths ranging between 43 to 52 MPa (Table 4). PLA from different sources demonstrated a wide range of properties. This is visually clear from observation of the results in Figure 2. While most PLA's exhibited similar Elastic Modulus of around 3GPa, considerable differences are observed for the other properties. PLA1 had very high UTS but the lowest ductility as noted by the lack of necking in the specimen. Similarly, no appreciable necking was observed in the gage section for test specimen of PLA2, PLA6, and ToughPLA. These are characterized by a high UTS (51.7 MPa), high stiffness (E=3.38 GPa), and low elongation (2.77%) prior to failure. By contrast, PLA/PHA1 and woodPLA demonstrated the lowest UTS of about 35 MPa and the highest elongation of nearly 6%.

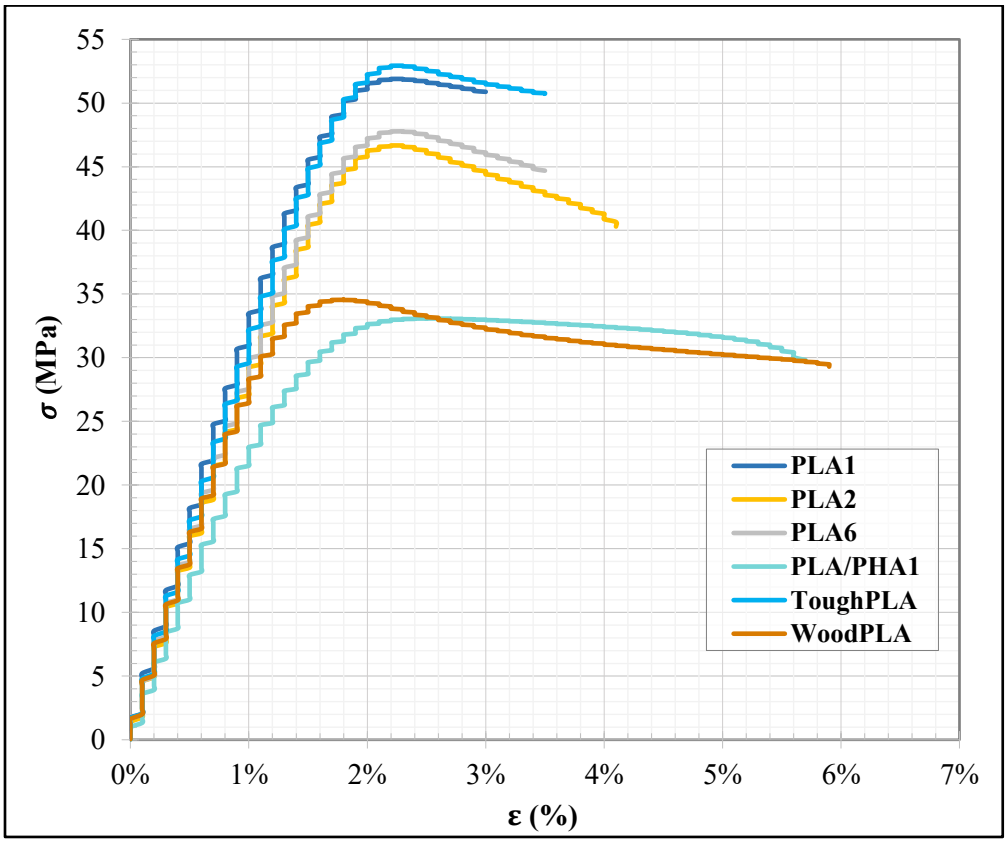

Figure 2. Raw stress-strain curves of select PLA-based samples

As shown in Figure 2, PLA1 is stronger and less ductile than PLA2 and PLA6. The difference in tensile performances of the six tested PLA materials may be affected by the color of the material, which has been investigated in other works (Wittbrodt & Pearce, 2015). The authors observed that natural, blue, and white colored PLA exhibited the greatest tensile stress and modulus compared to other colors (black and gray). Specifically, white colored PLA possesses high crystallinity which influences the mechanical properties of the material. The current work shows that the addition of colorants to PLA (PLA2 & PLA6) during the material manufacturing process results in a small reduction in the material strength compared to natural or uncolored PLA

(PLA1). A similar observation can be made for PLA6, based on the stress-strain behaviour (Fig.2), confirming that the addition of white colorant to PLA (PLA6) effectively decreases the strength of natural PLA (PLA1), whereas the difference in strength between white (PLA6) and gold (PLA2) PLA is minimal. The influence of color can be further evaluated by comparing the UTS of two white colored PLA materials obtained from different suppliers, as reported in Table 4. Although, PLA3 (43.5 MPa) and PLA6 (47.3 MPa) did not have the highest strength of all PLA-based materials, they exhibited the lowest fracture strain.

The stress strain curve for PLA/PHA1 (Fig. 2) shows that a blend of co-polymers results in improved material ductility and toughness but at the expense of strength. A characteristic flattening of the stress strain curve at the yield point is noted in PLA/PHA1, compared to the prominent yield points observed in the other curves presented in Figure 2. One interesting observation is the large difference in strengths between the two PLA/PHA blends tested, PLA/PHA1 (32.8 MPa) and PLA/PHA2 (48.6 MPa) (Table 4). Both blends were obtained from the same source. Unfortunately, the chemical composition of both materials is unknown. A comparison between the PLA/PHA blends can be made based on color, as previously discussed. The results show that samples printed from white colored PLA/PHA had much lower tensile strengths than green-colored PLA/PHA, the effect on fracture strain is negligible as the average values of both are within one standard deviation.

The results of the three modified PLA materials (SilkPLA, ToughPLA, AdvPLA) will be examined based on the results from Table 4 and Figure 2. The results show that specimen fabricated from ToughPLA reported to have the greatest tensile strength (53.3 MPa) and modulus (3.38 GPa) compared to the other PLA-based materials (see Table 4). This confirms the superior strength and toughness claimed for ToughPLA. In contrast, SilkPLA samples had the lowest stiffness (2.02 GPa) out of all PLA-based specimen, and experienced strains of over 45% prior to fracture, which is an order of magnitude higher than all other PLA materials. Under tensile testing conditions, the strength, modulus, and fracture strain of AdvPLA are within the standard deviation of values observed for all regular PLA tested samples (PLA1-PLA6).

Figure 3 shows the stress-strain curves for ABS, PETG, and Copolyester test samples. The linear elastic behavior of the two ABS materials was very similar: including overall strength (~35 MPa) and stiffness (2 GPa). However, large differences in fracture strain are observed after the maximum tensile stress is reached in both samples in the plastic region. The ABS1 stress-strain curve shows a slow decrease in stress followed by rapid fracture, whereas the ABS2 curve shows a characteristic drop in stress following the yield point prior to deformation of the neck region. The brittle fractured surface of ABS1 specimen are shown in Figure 4 (top left). No appreciable necking is observed and shear bands produced by yielding deformation are noted in the majority of tested specimens. Heavy crazing formation is present along the thickness of the fractured

samples causing whitening of areas surrounding the fracture site, indicated by red circled regions in Figure 4 (bottom left).

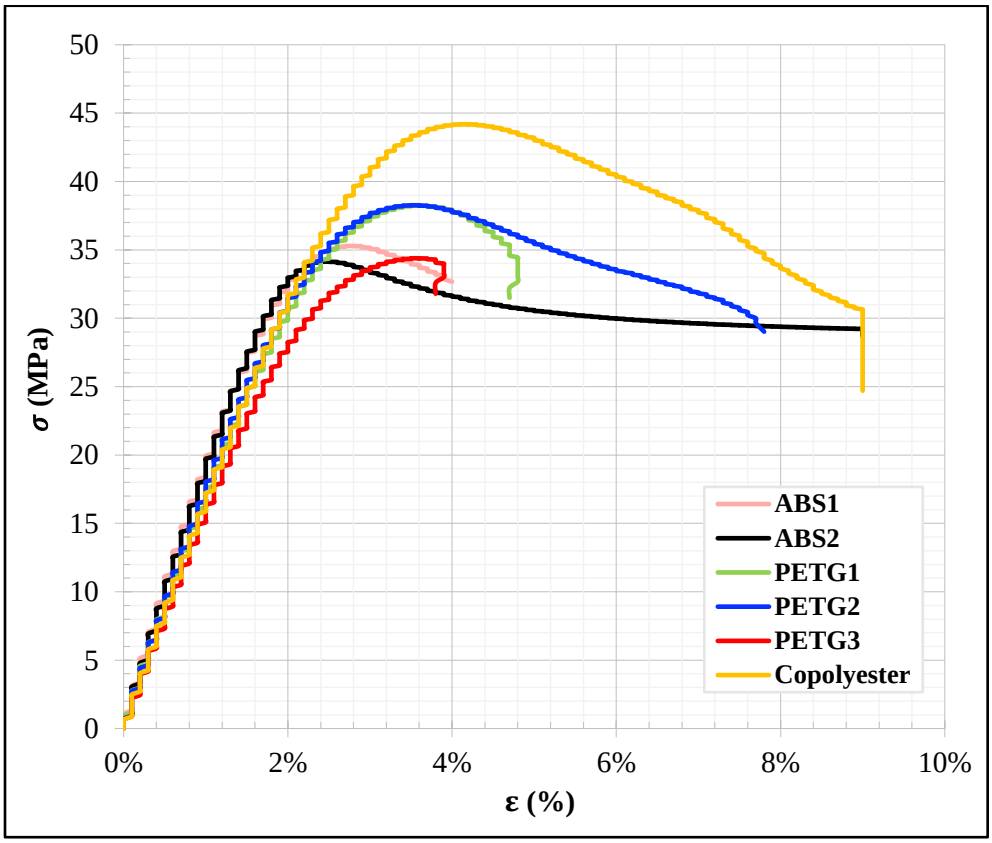

Figure 3. Raw stress-strain curves for ABS, PETG, and Copolyester test samples

It is evident from the general shape of the stress-strain curve for ABS2, that the specimen experienced drawing resulting in ductile failure. A clear yield point is present followed by a decrease in strength and drawing indicated by the substantial elongations within the plastic region of the curve with a slope approaching 0. Fracture of the ABS2 sample occurs at a low stress (~28 MPa) and large strain (~9 %) values, characteristic of a ductile failure. Table 5 indicates that on average, ABS2 samples fractured at a strain of 12.7 ± 6.8%, nearly four times that of ABS1 (3.7 ± 0.6%,). ABS2 specimen showed a large range of plastic deformation within the gauge length of the fractured samples (Fig 4, top right). No necking is visibly present on any of the specimen, though whitening along the gauge length of extremely warped specimen is noted (Fig 4, bottom right). The fracture sites are rough, sharp and occur normal to the applied stress. All specimen fractured inside or right on the edge of the gauge length. The discrepancies in elongation during tensile testing are likely a result of chemical composition of the filament or printing defects in the samples. Since the compositions of both ABS types are unknown, the difference in failure mode requires further analysis to accurately confirm the cause.

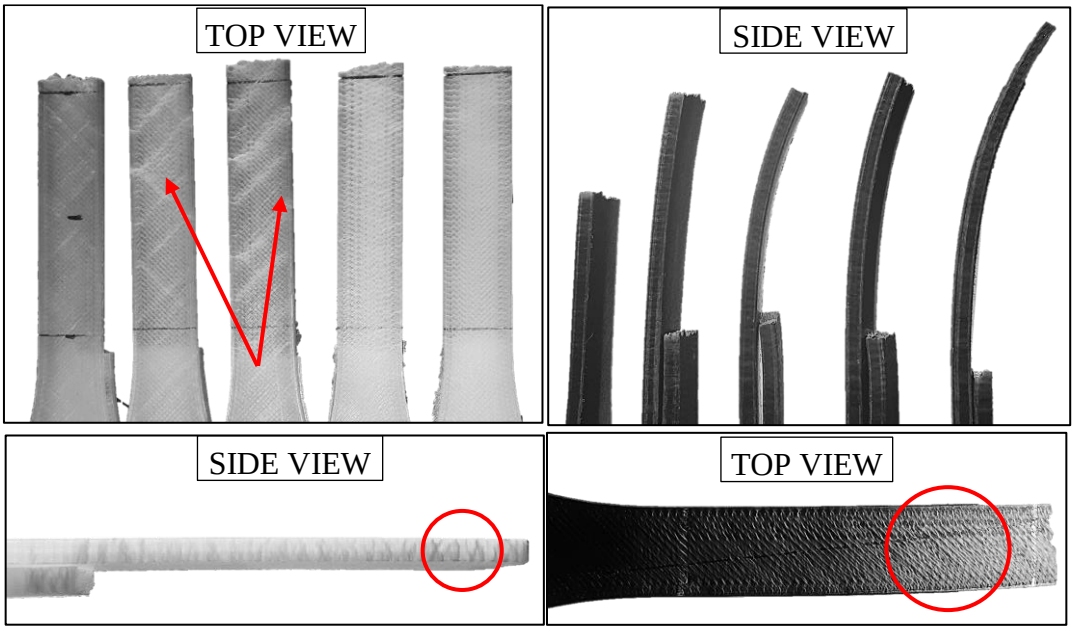

Figure 4. Fractured ABS1 (left) and ABS2 (right) test samples, showing shear banding (top left) and crazing formation (bottom left & right)

The stress-strain curves for PETG1, PETG2, PETG3, and Copolyester are also compared in Figure 3. The greatest strength at yield was exhibited by Copolyester (~44 MPa), followed by PETG2, PETG1, and PETG3 which reported UTS between 36-40 MPa. In addition to high strength, Copolyester samples were on average about twice as ductile (~11%) as the three other PETG samples. A combination of high strength and elongation prior to failure, evident from the stress-strain curve for Copolyester (Fig. 3), yielded a Copolyester with high toughness. The degree of elongation prior to failure observed for Copolyester is comparable to ABS2 (Fig 3), however the deviation reported in the value of fracture strain for Copolyester is significantly lower than ABS2. Visible signs of necking are present in all test specimen of Copolyester, a clear reduction of thickness can be seen in Figure 5 (bottom left), concentrated in areas surrounding the fracture site. The fracture site appears fibrous and dull (Fig 5, top left), indicating specimen failed in a ductile manner. Additionally, two of five test specimen had a small piece of filament break off from the failure region, indicated by the red arrow in Fig.5 (top left). The fractured surface of Copolyester shows that fracture in majority of specimen occurred at 45° angles to the applied tensile load. A similar mode of failure occurred in both PETG1 and PETG2. Both materials are comparable in performance, with average values within standard deviation of one another (Table 5).

Strain softening, indicated by a nonlinear drop in stress with increasing strain, occurs within the plastic region of the stress strain curve for PETG2 (Fig 3). As a result, evidence of shear banding deformation in multiple fractured specimen of PETG2 is presently seen in Figure 5 (top left). Evidence of strain softening is observed in both PETG1 and Copolyester samples as well.

PETG3 was the only PETG-based material to experience a brittle mode of failure, with no visible necking observed in fractured tensile samples. All tensile specimen of PETG3 failed outside of the extensometer gauge length and fractured normal to the applied load. Despite the characteristics associated with this mode of failure, PETG3 reported the lowest strength (35.9 MPa) and modulus (1.67 GPa), compared to others.

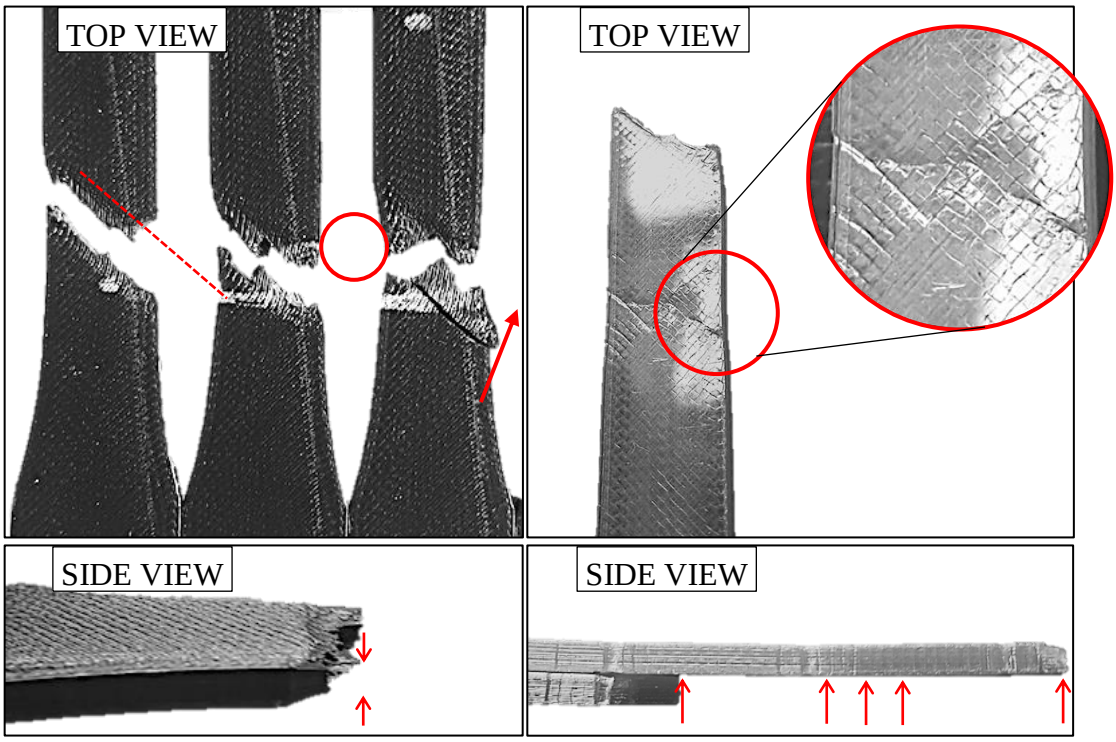

Figure 5. Copolyester (left) and PETG2 (right) fractured samples

Both Nylon materials possess high tensile strengths overall tested materials. Comparing between the two types, Nylon 2 is about 20% stronger (63 MPa) and stiffer (2.58 GPa) than Nylon 1 (Table 6). Nylon1, however, is much more durable and withstands six times more strain before failure (28.4%) compared to Nylon 2 (4.56%). ASA is similar in strength to both ABS1 and ABS2, however ASA test samples fractured at much lower strains compared to ABS. ASA filament printed with ease, no warpage was observed during printing due to excellent bed adhesion. PEI had a unique combination of properties. On one hand the high strength (59 MPa) and very low fracture strain (0.07%) is consistent with a highly brittle crystalline material. However, the modulus of PEI (1.53 GPa) is the lowest reported overall, indicative of a soft material with high performance capabilities. Finally, Polyolefin was the softest and weakest polymeric material tested.

4.2 Tensile Properties of Polymer Matrix Composites

The tensile results for the polymer matrix composite samples are listed in Table 7. The results show that the incorporation of wood fibers in PLA, yields a decrease in UTS, and modulus.

However, there is an increase in the fracture strain of wood-filled PLA compared to the six types of PLA tested (Table 4). The performance of glass-filled PLA is similar, however, glassPLA samples possess slightly higher tensile strengths and stiffnesses, compared to woodPLA. Comparing the two Cu-filled PLA materials, CuPLA1 and CuPLA2, there is a significant difference in performance between the two materials which were obtained from different sources. CuPLA1 reported the lowest tensile strength (~11 MPa) on average of all tested materials. The tensile strength of CuPLA2 samples were higher (22 MPa), however, both Cu-filled materials show a decrease in strength and increase in stiffness due to the addition of Cu particles, compared to the unfilled PLA materials tested (Table 4).

Table 7. Tensile results for polymer matrix composites 3D-printed materials

Name	UTS (MPa)	Strain at Max load (%)	Elastic Modulus (GPa)	Fracture Stress (MPa)	Fracture Strain (%)
WoodPLA	35.5 ± 1.4	1.78	3.06 ± 0.11	29.12	6.46 ± 0.59
GlassPLA	38.5 ± 0.2	2.04	3.27 ± 0.03	36.64	2.47 ± 0.24
CuPLA1	11.4 ± 0.6	1.51	3.63 ± 0.15	9.89	1.82 ± 0.61
CuPLA2	22.4 ± 1.6	1.16 ± 0.11	4.29 ± 0.45	19.5 ± 1.82	1.48 ± 0.27
CFPLA	15.1 ± 0.4	2.28	1.71 ± 0.04	2.77	49.8 ± 10.2
CFABS	37.3 ± 0.4	1.97	2.71 ± 0.03	33.44	6.06 ± 1.0

Finally, the stress-strain curves of the two carbon-fibre containing materials are shown in Figure 6. While the Elastic modulus, yield strength and UTS for each set of tested samples are highly reproducible, the strain to failure is extremely variable. It is clear from the curves that ABS is a more suitable polymeric binder for carbon fibres due to the stability in terms of failure of the samples shown by the clearly indicated regions of failure for CFABS samples compared to CFPLA samples.

4.3 Fracture toughness

The fracture toughness of some of the polymer and polymer matrix samples are shown in Figures 7 and 8 following ASTM D256. PLA4 and PLA5 were selected from Table 4 for fracture toughness evaluation as they demonstrated the best combination of UTS and strain at fracture. PLA5 is clearly yielded a higher fracture toughness than PLA4. Surprisingly, even though the composite CuPLA1, GlassPLA and CFPLA samples had lower UTS and strain to fracture than PLA4 and PLA5, their fracture toughness is comparable to the non-composite PLA samples. Finally, PLA4 was given several heat treatments after printing and before testing for toughness. The results are shown in Figure 8. Several heat treatments were evaluated: 55^{o}C for 1 hour, 70^{o}C for 1 hour and 70^{o}C for 5 hours. The 55^{o}C for 1-hour heat treatment resulted in no difference in fracture toughness compared to the non-heat treated PLA4 sample. However, a 70^{o}C for 1-hour heat treatment resulted in more than double the fracture toughness of the sample. This may be the result of increased crystallinity occurring during heat treatment. Longer times at 70^{o}C did not yield improved results. Thus, optimum properties of these polymeric and composite samples can to some degree be manipulated to levels beyond what is received and printed.

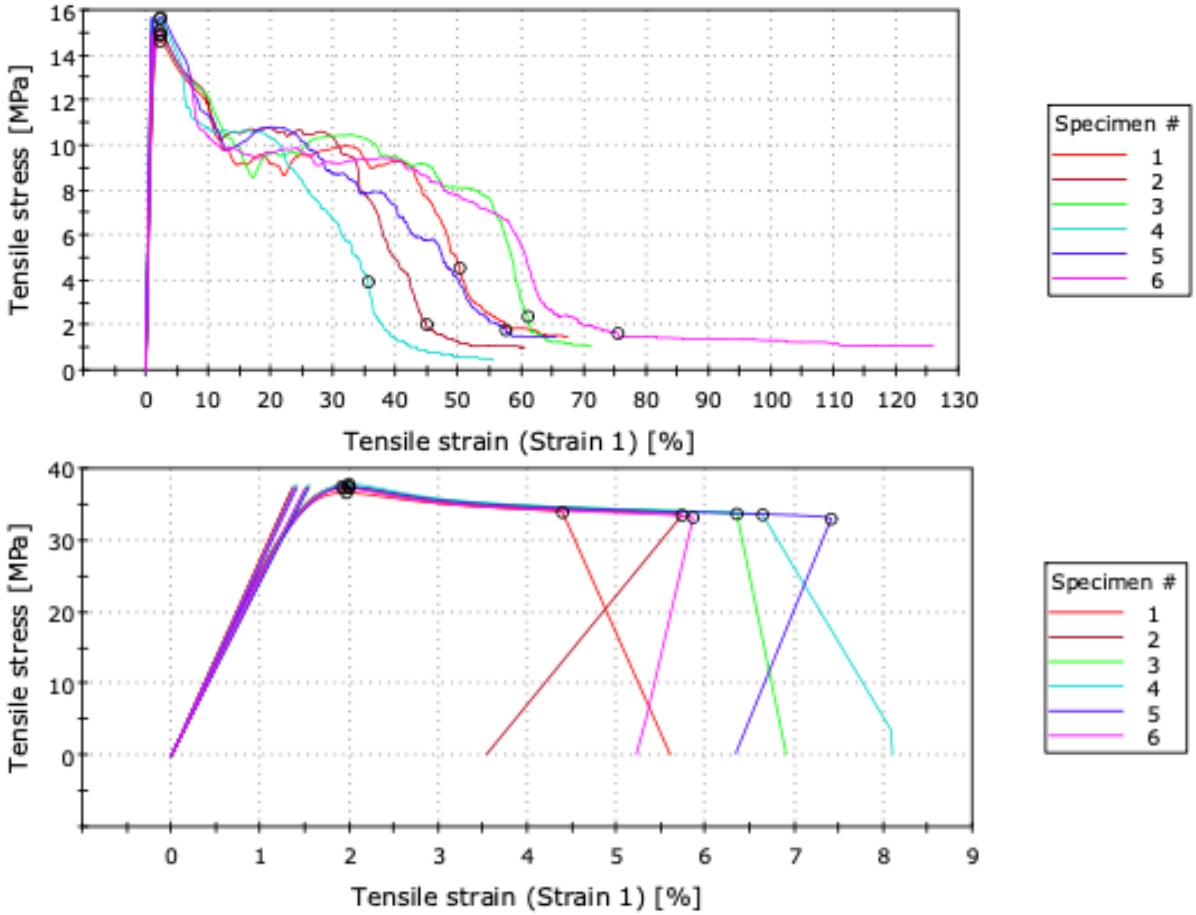

Figure 6. Raw stress-strain curves for CFPLA (above) and CFABS (below)

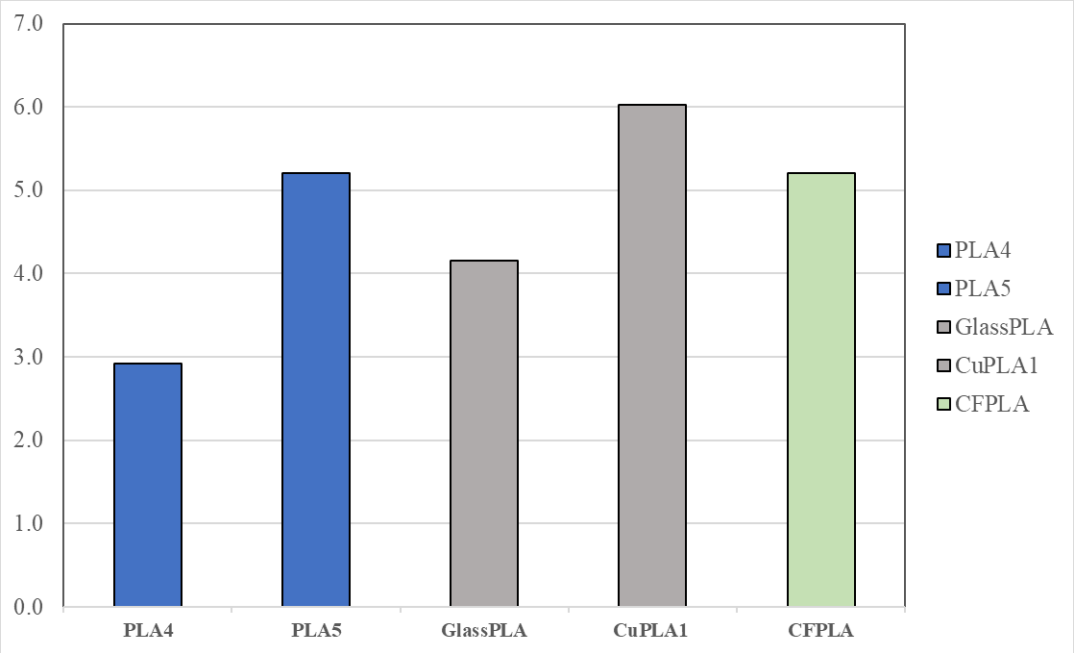

Figure 7: Fracture toughness of several 3D printed materials.

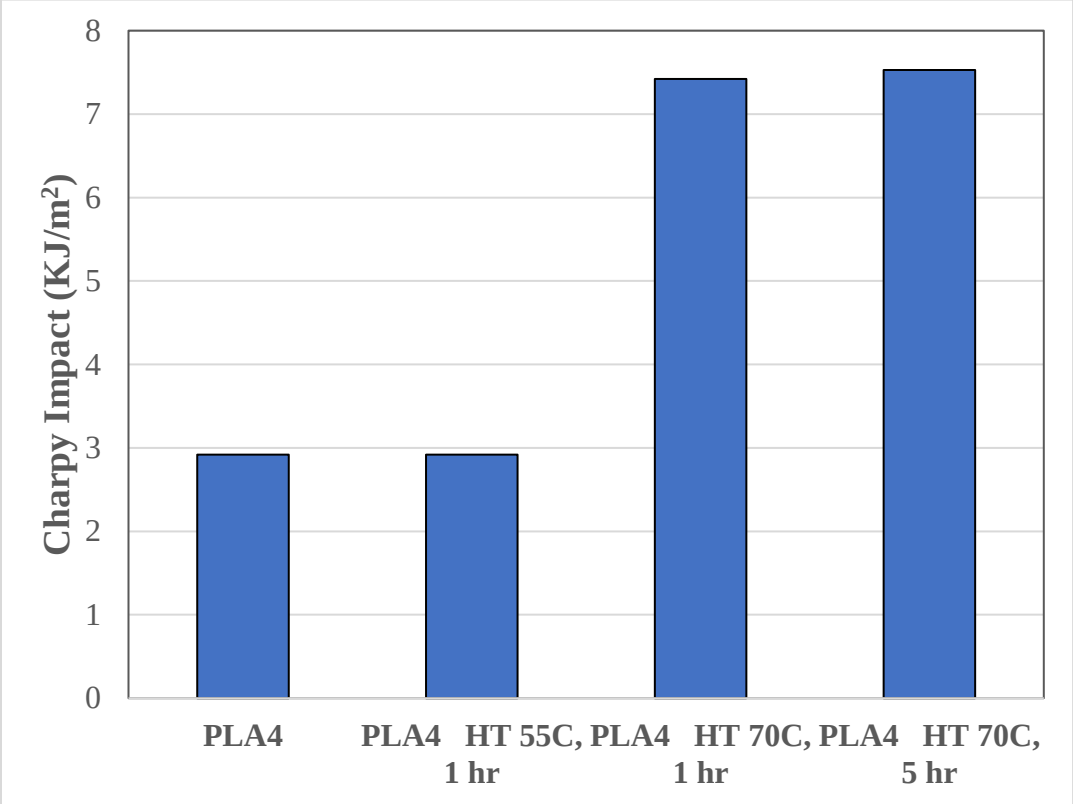

Figure 8: Fracture toughness of several 3D printed materials comparing the effect of heat treatment.

5. Conclusions

Tensile testing was conducted to characterize and compare the mechanical properties of various polymer filaments, commonly used in FFF or 3D printing. This data is critical to gain commercial acceptance of the technology in industrial applications. The tensile properties were assessed based on failure under tensile loading and in fracture toughness. Experimental results of this study serve as a basis for material selection for 3D-printing applications. It is clear that if using polymeric filaments in FFF processing for engineering applications, the properties of the supplied filaments need to be evaluated by the user beyond the supplied datasheets. Variations in properties are clearly apparent and can be manipulated subsequent to printing by heat treatment. The mechanical properties of various printable materials allow the selection of the appropriate material for the desired application.

Acknowledgements

The authors wish to acknowledge the funding of this work from the Natural Science and Engineering Research Council and the support provided by InnoTech Alberta where some of the experiments were carried out.

References

(ASTM, 2014) ASTM International. D638-14 Standard Test Method for Tensile Properties of Plastics. West Conshohocken, PA; ASTM International, 2014. doi: https://doi-org.login.ezproxy.library.ualberta.ca/10.1520/D0638-14

(Górski et al., 2013) Górski, F., Kuczko, W., & Wichniarek, R. (2013). INFLUENCE OF PROCESS PARAMETERS ON DIMENSIONAL ACCURACY OF PARTS MANUFACTURED USING FUSED DEPOSITION MODELLING TECHNOLOGY. Advances in Science and Technology, 7, 9.

(Bellini & Güçeri, 2003) Bellini, A., Güçeri, S. (2003),"Mechanical characterization of parts fabricated using fused deposition modeling", Rapid Prototyping Journal, Vol. 9 Iss 4 pp. 252 – 264

(Rothon et al., 1996) Rothon, R.N., DeArmitt, C, Hancock, M. (1996) Particulate-Filled Polymer Composites 2nd Edition Ch.8, Rapra Technology Limited 357 – 413

(Wittbrodt & Pearce, 2015) Wittbrodt, B., & Pearce, J. M. (2015). The effects of PLA color on material properties of 3-D printed components. *Additive Manufacturing*, *8*, 110–116. https://doi.org/10.1016/j.addma.2015.09.006

(Callister, 2009) Callister, W., *"Material Science and Engineering: an Introduction",* ed. 8th, 2009

(Schultz, 1974) Schultz, "*Polymer Materials Science",* ed. 1, 1974

(Droste & Dibenedetto, 1969) Droste, D.H. and Dibenedetto, AT. (1969) The glass transition temperature of filled polymers and its effect on their physieal properties, J. Appl. Polym. Sei., 13,2149-68.

(Johnson & French, 2018) Johnson, G. A., & French, J. J. (2018). Evaluation of Infill Effect on Mechanical Properties of Consumer 3D Printing Materials. 3(4), 6.